Electronic Supplementary Material (ESI) for Journal of Materials Chemistry C

Cellulose Nanofibers Decorated with Magnetic Nanoparticles – Synthesis, Structure and Use in Magnetized High Toughness Membranes for a Prototype Loudspeaker

Sylvain Galland, Richard L. Andersson, Michaela Salajková, Valter Ström, Richard T. Olsson and Lars A. Berglund

SUPPLEMENTARY INFORMATION

Supplementary Methods

Extraction of cellulose nanofibrils from wood pulp

Commercial pulp (Nordic Paper, Sweden) with hemicellulose and lignin contents of 13.8% and 0.7%, respectively, was used as starting material. The degree of polymerization (DP) of the cellulose was ca. 1200. The cellulose nanofibrils were extracted following a previously reported procedure[1], involving enzymatic pre-treatment at 50 °C for 2h in an aqueous solution of the enzyme endoglucanase Novozyme 476) at 0.25% (0.1 mL enzyme / 40g dry content cellulose). The enzymatic treatment was followed by 8 passes through a M–110EH microfluidizer (maximum pressure 1100 bar, Microfluidcs Ind., USA) applying sufficient shear forces to liberate the cellulose fibrils from their agglomerated state. An aqueous nanofibril cellulose gel suspension with 1.6 wt.% solid content was obtained. The nanofibril suspension was diluted to 0.3 wt.% in 1.2 L of distilled water (MilliQ, Millipore, USA), and then subjected to ultrasound (Vibracell VCX 750, Sonics, USA) twice for 5 minutes at 225 W in order to improve the dispersion and liberation of the individual nanofibrils.

Membrane preparation by vacuum filtration

Large magnetic cellulose membranes (20 cm diameter) were made from the in-situ prepared magnetic cellulose nanofibrils by vacuum filtration and further drying in a vacuum oven at 93 °C (Rapid-Köthen, Frank-PTI, Germany) as reported by Sehaqui et. al.[2] The magnetic nanofibril suspensions were diluted to 0.2 wt.% and high-shear mixed for 10 min, followed by filtration on a 0.65 μm pore size membrane (Millipore, USA). Membranes with a uniform thickness in the range of 50–60 μm were obtained.

For comparison, separately precipitated nanoparticles in suspensions were mixed with different amounts of unmodified NFC to prepare membranes with the same fractions of nanoparticles as in the case of in-situ modified nanofibrils (10, 30 and 60 wt.% inorganic phase). In addition, a 0 wt.% inorganic phase reference membrane was obtained by subjecting the cellulose nanofibril suspension to the same alkaline conditions as in the co-precipitation reaction but in absence of metal salts, the pH being held at 10 by the addition of NaOH and KNO_3 during 6 h.

Thermogravimetric analysis of the magnetic membranes

Samples from the different membranes were analyzed in a thermogravimetric analyzer (Mettler-Toledo, TGA/SDTA851, Switzerland) under a 50 ml/min O_2 flux. The heating rate was 10 °C/min. After a first ramp to 100 °C, the temperature was held for 10 min to remove loosely bound residual water in the samples, followed by a second ramp to 120 °C, and another 10 min at this temperature to eliminate strongly bound residual water. The dry mass at 120 °C was taken as the reference. The analysis was completed by a third ramp up to 550 °C to ensure complete degradation of the cellulose material.

Mechanical testing at different humidity conditions

Thin strips (5 x 50 mm) of the membranes were tested in a mechanical tensile testing system (Instron 5944) at 23 °C and 50 %RH according to the ASTM D882 standard. The strip thickness and width were measured with a thickness meter (Mitutoyo, Japan) and a micrometer, respectively. The gauge length was set to 25 mm and the crosshead displacement was 10 % per min. At least 6 specimens were tested at each experimental condition. A first set of specimens was conditioned for 2 weeks in a regulated climate room (23 °C, 50 %RH) before testing. Another two sets were placed in chambers below 5 %RH and above 95 %RH, respectively, for 2 weeks conditioning before testing.

The density of the materials was obtained from thickness, mass and area measurements (from image analysis of black and white photographs). The porosity was calculated assuming cellulose nanofibril and cobalt-ferrite nanoparticle densities of 1460[3] and 4900[4] $kg.m^{-3}$, respectively.

Scanning and transmission electron microscopy

Field-emission scanning electron microscopy (FE-SEM, Hitachi S-4800, Japan) was used to observe cross-sections of the fractured membranes and individual functionalized nanofibrils. A ca. 3 nm gold-palladium layer was sputtered (Cressington 208HR, UK) onto the samples to reduce electrical charging of the cellulose nanofibrils. The functionalized nanofibrils were studied as deposited on a mica substrate prepared as a layer–by–layer assembly. A positively charged 0.1 wt.% poly-l-lysine (Ted Pella, USA) layer was first deposited on the cleaved mica substrate by applying a drop of the polymer solution 3 min on the surface, followed by rinsing with distilled water and drying under a gentle N_2 flow. The procedure was repeated with a suspension of functionalized nanofibrils diluted to ca. 0.001 wt.%, and sonicated for 20 s at 150 W. The negative charges present at the surface of the cellulose nanofibrils and ferrite nanoparticles ensured deposition and anchoring / attachment to the mica surface.

Transmission electron microscopy (TEM, Hitachi HT7700, Japan) was used to determine particle size distributions for the different reactions (manually determined from at least 500 nanoparticles). The modified cellulose nanofibrils from the as-prepared suspension or separately prepared ferrite nanoparticles were sonicated before deposition on TEM grids (ultra-thin carbon film / holey carbon – 400 mesh, Ted Pella, USA).

Magnetic characterization of the membranes

The magnetic characterization was performed in a vibrating sample magnetometer (VSM, Oxford Instruments, UK). The applied magnetic field strength was varied in the range of ± 500kA/m and the measurements were performed on thin strips (10 x 2 mm) from the prepared membranes (initially demagnetized). Data were normalized to the mass of nanoparticles (derived from thermal gravimetric analysis, TGA).

X-ray diffraction

The X–ray diffraction was performed on a PANalytical X'pert Pro MPD. For all measurements, Cu-K_α radiation ($\lambda = 154.2$ pm) was used. Due to the strong fluorescence of the ferrite, a setup with a parabolic mirror and a secondary monochromator was used. The analysis was performed on the unaltered diffraction patterns, *i.e.* no smoothing or background correction was applied. All data collections were taken at ambient temperature (24 °C).

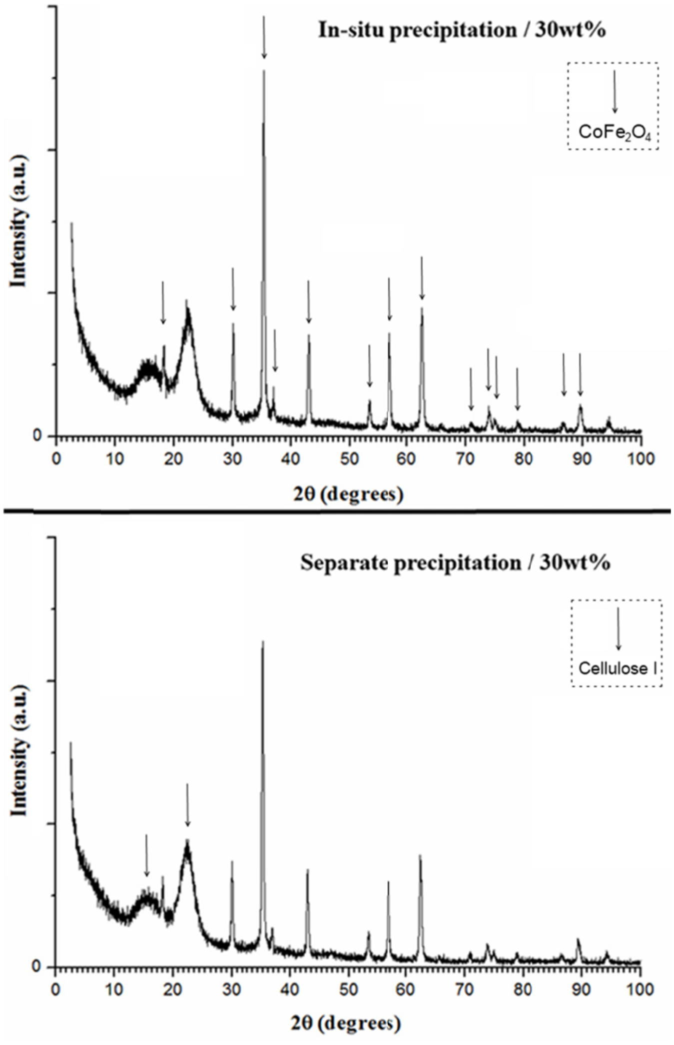

Figure S1. X-ray diffraction pattern of magnetic NFC hybrid membranes with 30 wt.% of cobalt-ferrite, prepared by in-situ precipitation (top) and separate precipitation plus mixing (down). Peaks are assigned to the constituents as indicated in the graphs.

The X-ray diffractograms for the 30 wt.% hybrid composite membranes are shown in Fig. S1. All the hybrid cellulose/nanoparticle samples exhibited the characteristic peaks corresponding to a clean spinel cobalt-ferrite phase and, at small diffraction angles, also the peaks corresponding to cellulose I. The diffraction patterns revealed no trace of any oxo-hydroxide phase, confirming that the conversion into the spinel phase was completed. A more thorough analysis of the spectra showed no significant variations in the lattice parameter of magnetic crystals for the different samples in the vicinity of 842 pm. The relative amplitude of the cellulose and cobalt-ferrite peaks depended on the nanoparticle content of the sample.

Table S1. Results of metal salts adsorption study on cellulose fibrils from ICP-OES analysis

Aimed	Introduced	Adsorbed at room temperature			Precipitated oxo-hydroxides at 90°C		
$CoFe_2O_4$ content (wt.%)	total metal introduced (mmol/g_{cell})	Metal amount (mmol/g_{cell})	mol.% of introduced amount	occupied % of cellulose sites	metal amount (mmol/g_{cell})	mol.% of introduced amount	wt.% of metal on fibril
10	2	0.04	1.8	2.7	0.20	10.1	1.8
60	20	0.20	1.0	15.7	0.33	2.0	3.0

Table S1 shows the amount of metal cations (iron and cobalt) adsorbed and precipitated as oxo-hydroxide precursors onto the cellulose surfaces in the 10 wt.% and 60 wt.% systems. The initial metal ion suspension contained ca. 2 and 20 mmol of metal cations per gram of cellulose nanofibrils, respectively. (The ratios refer to conditions for the “in-situ” preparations of hybrid fibrils for the membranes.) Only a few per cent of the total metal ion content in the suspensions were adsorbed onto the nanofibril surfaces (ca. 2 and 1 mol.%, respectively). In the more concentrated system, this amount corresponded to about 15 % of the calculated available adsorption sites at the cellulose surface, and to 3 % of the sites in the more dilute system. The calculation of theoretical number of adsorption sites is described below.

The rather low occupancy of adsorption to the calculated theoretical sites in the more dilute system, referred to as “10 wt.%”, was related to the statistically smaller crowding of metal cations in the solution, naturally limiting the probability of adsorption to the surface. In the more concentrated system (“60 wt.%”), where metal ion complexes were in significant excess of the maximum theoretical number of available hydroxyl sites, the fraction of sites occupied was, however, still low, i.e. 15 % of the theoretical number. This limitation may relate to intra-molecular cellulose hydrogen bonds within, and possibly between, the cellulose fibers, which may have reduced the accessibility of surface located hydroxyl groups. However, upon heating to 90 °C, 0.20 and 0.33 mmol of metal cations were precipitated onto the fibers in the form of solid oxo-hydroxide rods.

Calculation of theoretical number of adsorption sites at the fibril surface

The average lateral dimension of the cellulose nanofibrils used in this work was about 9 nm. This corresponds to a total specific surface area of 300 m^2/g, considering perfectly square cross-sections and neglecting surfaces exposed at the extremities of the fibrils (assuming aspect-ratio >100).[1,5] The area of each hydroxyl group can be calculated based on established models of the cellulose I crystalline structure.[6] The unit cell has dimensions of ca. 1 and 0.56 nm in the longitudinal and lateral directions, respectively. The unit cell contains one cellobiose unit which, if it lies on the fibril surface, results in 3 available hydroxyl groups. The estimated average area of one surface hydroxyl group is therefore $1 \times 0.56 / 3 = 0.187\ nm^2$. Considering that a divalent metal cation would adsorb to a pair of hydroxyl groups, the theoretical number of adsorption sites is $300 / 0.187 \times 10^{-18} / 2 = 2.68 \times 10^{20}$ sites per gram of cellulose, which can be converted to 1.33 mmol/g.

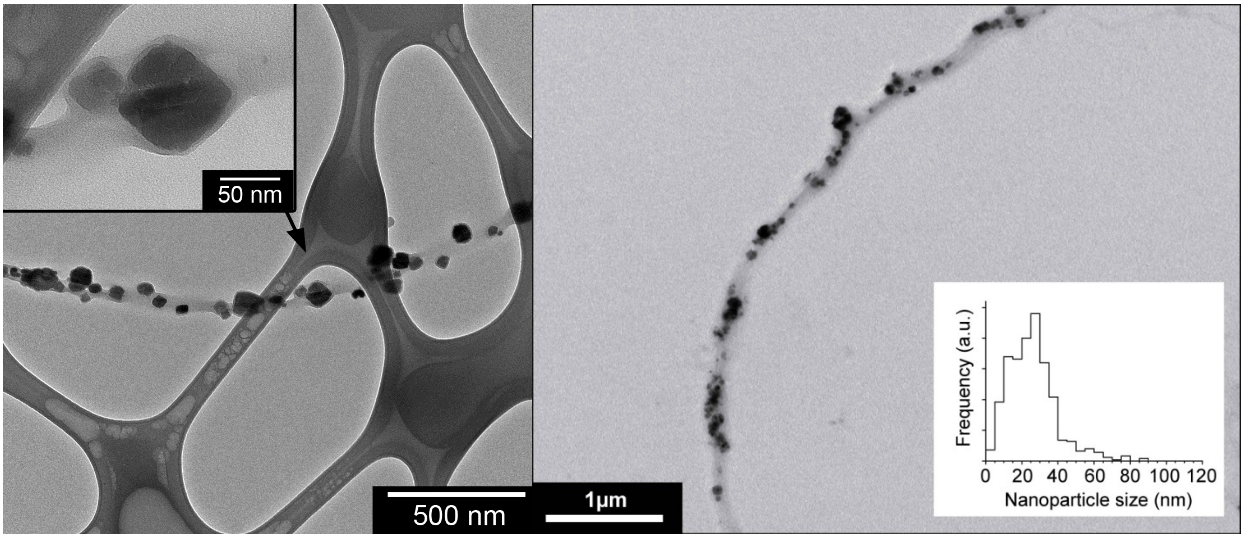

Figure S2 Left. TEM micrographs showing encapsulation of the magnetic nanoparticles in between merged fibrils, with inset enlargement. **Right.** TEM micrograph of a cellulose nanofibril decorated with $MnFe_2O_4$ nanoparticles (30 wt.%). Inset shows the particle size distribution obtained from image analysis of micrographs (manual counting of > 500 particles).

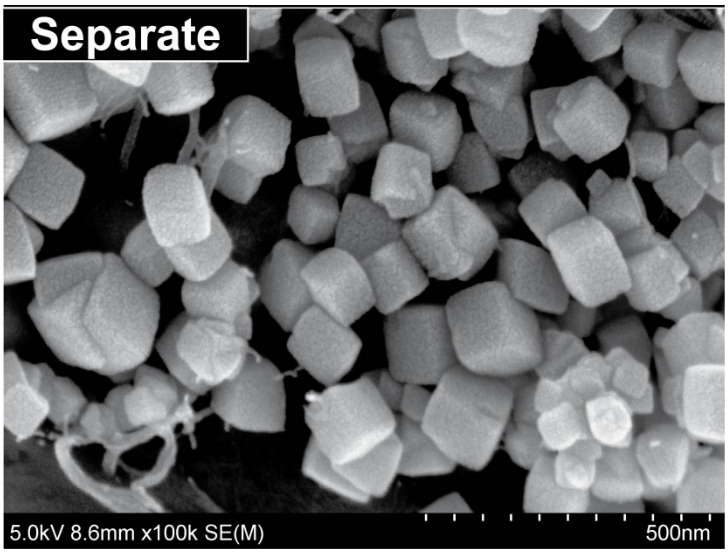

Figure S3. High-resolution SEM micrographs of nanoparticle precipitated in the absence (“separate”) of cellulose nanofibrils as located in a pocket observed in the cross–section of a membrane prepared by simply mixing pre–made particles with native cellulose fibers. The micrograph highlights the cubic morphology of the particles precipitated in the absence of nanofibrils.

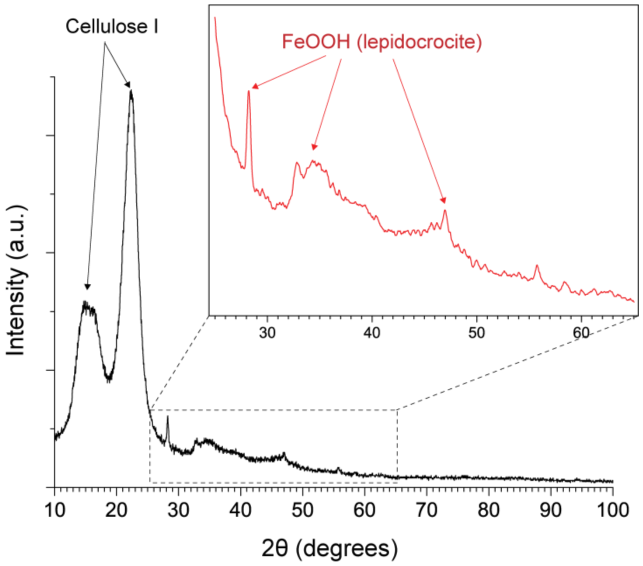

Figure S4. Cu K_α – X-ray diffraction pattern of an aliquot taken after heating the NFC/metal salts system prior to the enforced precipitation. The inset picture magnifies the peaks associated with the oxo-hydroxide phase that corresponded to 2–3 wt.% of the total cellulose mass during nucleation to the fibers.

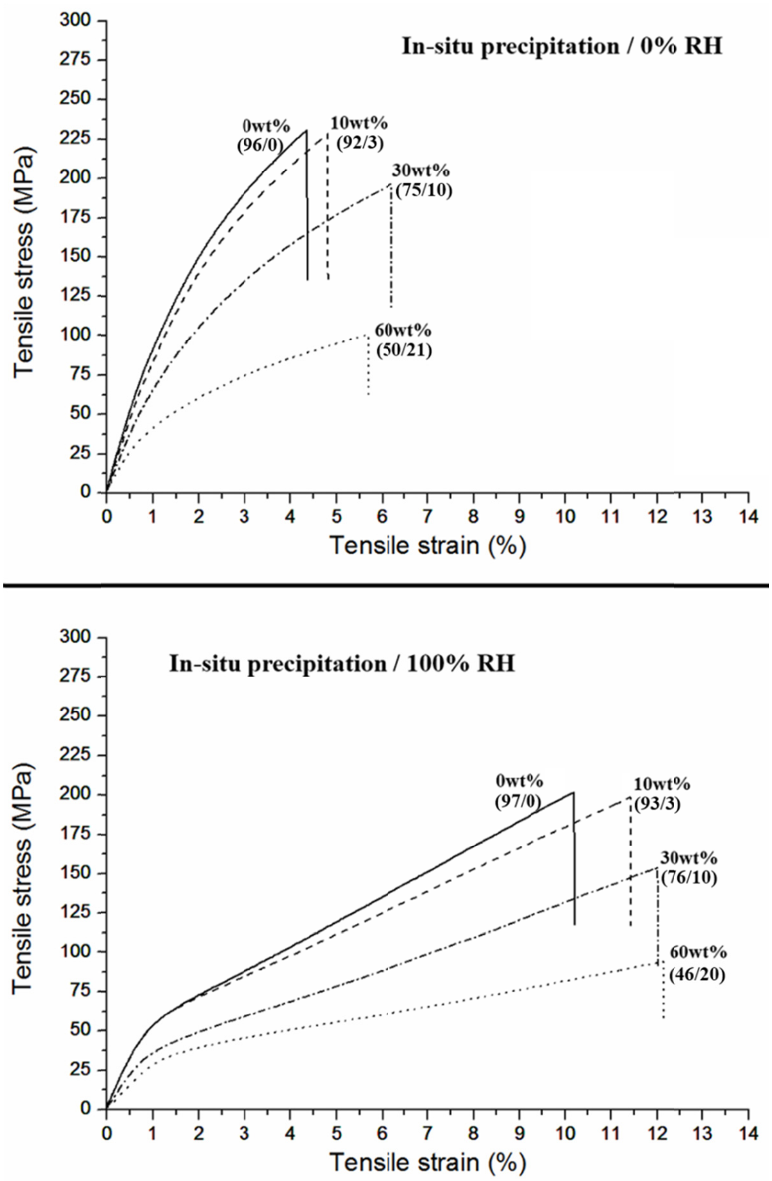

Figure S5. Representative tensile stress-strain curves for hybrid nanocomposite membranes based on decorated cellulose nanofibrils, with pre-conditioning below 5 %RH and above 95 %RH. In brackets the volume fractions of cellulose/nanoparticles.

Figure S4 shows the effect of moisture/water uptake on the mechanical properties of the in-situ prepared hybrid magnetic membranes. The uptake effects were assessed by performing the mechanical tests (stress-strain measurements) after sample conditioning at different relative humidity. The trends were independent of the amount of nanoparticles introduced, showing a stiffer and more brittle material in the dry state and a softer and more ductile material after conditioning at high relative humidity. Water molecules acted as plasticizing molecules in the cellulose nanofibril network by influencing inter–fibril hydrogen bonding and reducing nanofibril interactions. High strength was preserved due to stress transfer between the long and slender physically entangled nanofibrils, regardless of moisture uptake.

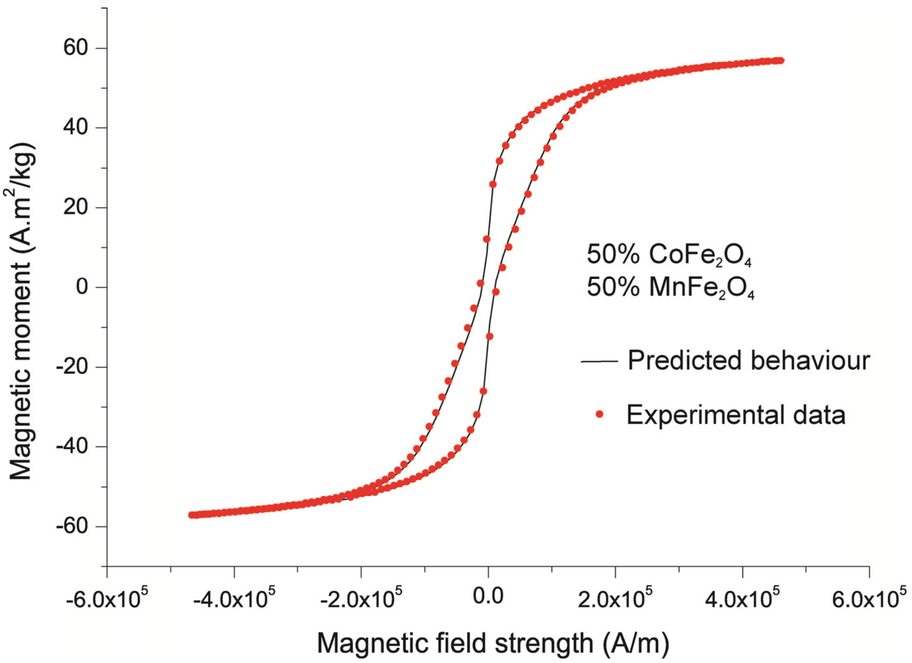

Figure S6. Experimental and predicted (Eq. 1) hysteresis magnetization curve for the nanocomposite containing 50 wt.% $CoFe_2O_4$ and 50 wt.% $MnFe_2O_4$–decorated cellulose nanofibrils.

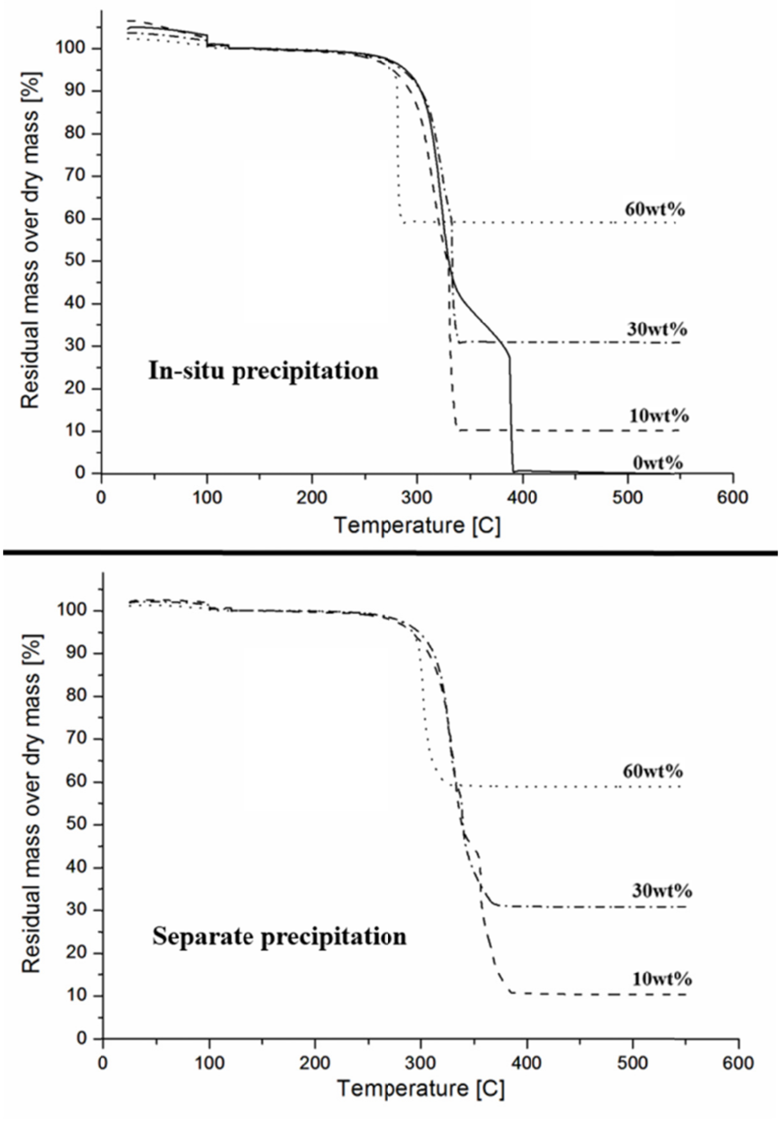

Figure S7. Thermal degradation curves for samples with different amounts of nanoparticles.

Thermogravimetric measurements were carried out at a heating rate of 5 °C per min under oxygen to confirm the nanoparticle contents in the membranes (Fig.S4). The degradation of the cellulose started at ca. 250°C and was completed above 350 °C. The nanoparticle content was calculated based on the residual mass above 400 °C.

Supplementary Video and Audio files

The video was recorded while pouring an aqueous suspension of decorated nanofibrils (3 wt.% dry content / 30 wt.% $CoFe_2O_4$ nanoparticles), demonstrating the colloidal “gel-like” material characteristics and its shaping possibilities.

The music recordings were made under the conditions described in the Method section of the paper, with the only difference that the microphone was changed to a DPA 4003 omnidirectional condenser microphone (Brüel & Kjaer, Denmark).

References

1 M. Henriksson, G. Henriksson, L.A. Berglund, T. Lindström, *Eur. Polym. J.,* **2007**, *43*, 3434.
2 H. Sehaqui, A. Liu, Q. Zhou, L.A. Berglund, *Biomacromolecules* **2010**, *11*, 2195.
3 C. Sun, *J. Pharm. Sci.* **2005**, *94*, 2132.
4 R.T. Olsson, G. Salazar-Alvarez, M.S. Hedenqvist, U.W. Gedde, F. Lindberg, S.J. Savage, *Chem. Mater.*, **2005**, *17*, 5109.
5 H. Sehaqui, Q. Zhou, L.A. Berglund, *Compos. Sci. Technol.*, **2011**, *71*, 1593.
6 Y. Nishiyama, P. Langan, H. Chanzy, *J. Am. Chem. Soc.*, **2002**, 124, 9074.